J. Phys. D: Appl. Phys. **46** (2013) 385303 (4pp) doi:10.1088/0022-3727/46/38/385303

Epitaxial stabilization of ultra-thin films of $EuNiO_3$

D Meyers[1], E J Moon[1,5], M Kareev[1], I C Tung[2], B A Gray[1], Jian Liu[1,3,6], M J Bedzyk[2], J W Freeland[4] and J Chakhalian[1]

[1] Department of Physics, University of Arkansas, Fayetteville, AR 72701, USA
[2] Materials Science and Engineering, Northwestern University, Evanston, IL 60208, USA
[3] Advanced Light Source, Lawrence Berkeley, Berkeley, CA 94720, USA
[4] Advanced Photon Source, Argonne National Laboratory, Argonne, IL 60439, USA
[5] Department of Materials Science and Engineering, Drexel University, Philadelphia, PA 19104, USA
[6] Department of Physics, University of California, Berkeley, CA 94720, USA

E-mail: dmeyers@uark.edu

Received 13 May 2013, in final form 1 August 2013
Published 4 September 2013
Online at stacks.iop.org/JPhysD/46/385303

Abstract
We report on the synthesis of ultra-thin films of highly distorted $EuNiO_3$ (ENO) grown by interrupted pulse laser epitaxy on $YAlO_3$ perovskite (YAP) substrates. Samples were then investigated with reflection high energy electron diffraction, atomic force microscopy, x-ray diffraction, reciprocal space mapping, and x-ray absorption spectroscopy. Combined, the measurements revealed the samples exhibited high structural and electronic quality that is of critical importance to the observed electronic and magnetic properties of the rare-earth nickelates. Growth of ultra-thin films of this highly distorted nickelate system in precisely controlled environments provides the ability to thoroughly investigate electronic phases with decoupled metal-to-insulator/charge-order and anti-ferromagnetic transitions.

(Some figures may appear in colour only in the online journal)

Complex transition metal oxides with correlated carriers are characterized by strong coupling between lattice, charge, spin and orbital degrees of freedom often resulting in emergent electronic and magnetic behaviours and strong collective response to weak external perturbation [1, 2]. Experimental investigation of their interesting properties ranging from high temperature superconductivity, exotic magnetism, and temperature driven metal–insulator transitions (MITs), however, relies on the availability of single crystal compounds. Furthermore, the availability of quality ultra-thin films adds another important dimension for developing theoretical models on how chemical composition, crystal symmetry and epitaxial relation between film and substrate translates into electronic and magnetic structures [3–5].

Recently, ultra-thin films of rare-earth nickelates $RENiO_3$ (RE = La, Pr, Nd, etc) have been actively synthesized and investigated [3, 6–15] motivated by theory-predicted exotic phenomena that may occur in ultra-thin films [16–18] and heterostructures [19, 20]. Bulk rare-earth nickelates are characterized by a small charge-transfer gap; all family members, except for the least distorted $LaNiO_3$, exhibit an MIT at a temperature designated T_{MIT} accompanied by long range charge order and unusual E'-type anti-ferromagnetic order at T_N [21, 22]. The MIT has proven to be highly tunable by epitaxial strain, pressure, carrier doping, and quantum confinement giving promise for future device applications [9, 23–27]. It is interesting to note that for Nd and Pr these transitions occur at the same temperature $T_N = T_{MIT}$ [28] while for smaller rare-earth ions (e.g. Eu, Y, Lu) the magnetic transition is well separated from the MIT and structural transition by a large temperature gap. This energy scale separation offers a unique opportunity to investigate these electronic phases separately, disentangling the effects of the charge and spin ordering to clarify the nature of both phases and verify very recent theoretical models [29–31].

In the bulk above T_{MIT} $EuNiO_3$ (ENO) has a strongly distorted orthorhombic structure (space group *Pbnm*) due to the relatively small size of the Eu ion. In this structure, the NiO_6 octahedra tilt to fill in the extra space due to steric effects, changing the Ni–O–Ni bonding angle and bonding length [32]. The larger Ni–O–Ni bond angle deviation from 180° narrows the 3D bandwidth W, causing the MIT to shift to higher

 © 2013 IOP Publishing Ltd Printed in the UK & the USA

temperatures. Thus the MIT in ENO shifts to around 460 K with magnetic ordering occurring below 210 K. Previous ENO studies have demonstrated that a charge disproportionation on the Ni 3d sites exists below the MIT [33]. The MIT has also been found to be tunable via external pressure in several other rare-earth nickelates, including ENO and $YNiO_3$ [27].

From the growth perspective, owing to the low thermodynamic stability of the nickelates, conventional solid state chemical synthesis requires very high oxygen pressure and temperatures and typically yields only *micron* sized single crystals [34–37]. This in turn has severely limited our understanding of the physics of these interesting compounds making thin film synthesis the most promising avenue to overcome these obstacles; even in thin film form these materials have thus far proven difficult to fabricate in a layer-by-layer fashion, becoming arduous upon application of strain [38]. Several recent publications detail the attempted growth of thin film nickelates by metal-organic chemical vapour deposition and sputtering [39–42]; for example, thick (∼210 nm) ENO films have been grown by rf magnetron sputtering resulting in an essentially low-quality textured morphology [43].

Here, we report on the growth of high quality, fully epitaxial ultra-thin films (15 unit cells (uc) or 5.86 nm) of ENO on YAP substrates in a layer-by-layer mode to epitaxially stabilize the RE nickelate films. Several characterization techniques revealed high chemical and structural quality, fully strained ultra-thin films of ENO synthesized for the first time to our best knowledge.

ENO (psuedocubic bulk lattice constant (BLC) = 3.80 Å) was grown on YAP (1 1 0) oriented substrate (psuedocubic bulk lattice constant = 3.71 Å; lattice mismatch −2.4%) by interrupted pulse laser epitaxy method using a KrF excimer laser (λ = 248 nm) with rapid pulse cycling of 18 Hz with typical pulse trains of 18 shots (∼1 s per unit cell); details of this growth mode can be found elsewhere [44, 45]. This approach allows for layer-by-layer growth which was confirmed by the presence of sharp specular intensity drops (during the pulse train) followed by total recovery monitored *in situ* by high pressure reflection high energy electron diffraction (HP-RHEED). After deposition films were annealed in 1 atm of ultra-pure oxygen for 30 min. The conditions best suited for layer-by-layer growth and high morphological quality for ENO were found to be ∼610 °C, P_{O_2} = 100–150 mTorr, and a laser power density varied between 2.2 and 2.4 J cm^{-2}. The film quality was investigated with reflection high energy electron diffraction (RHEED), atomic force microscopy (AFM), x-ray diffraction (XRD), reciprocal space mapping (RSM), and synchrotron based resonant x-ray absorption spectroscopy (XAS). Transport properties for these films were also investigated, and can be found elsewhere [46].

Figure 1(*a*) shows the characteristic time dependent specular intensity. As seen, during the rapid pulse sequence (typically ∼1 s) the RHEED intensity sharply drops and then rapidly recovers within a prolonged dwell time, characteristic of layer-by-layer growth. The lack of significant overall dampening of the intensity after multiple layers attests to

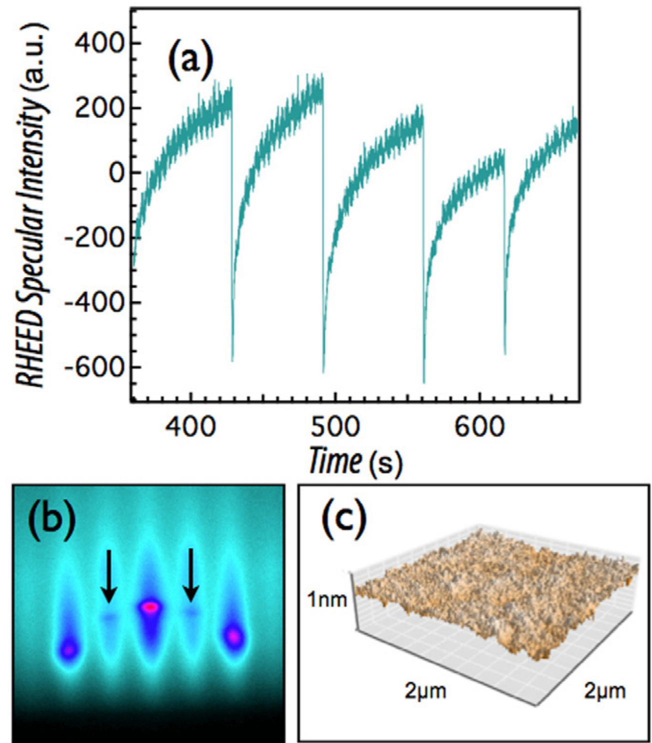

Figure 1. (*a*) RHEED specular intensity taken during growth of 15 uc ENO on YAP. (*b*) RHEED pattern of the 0th Laue circle on the same ENO sample, black arrows indicate the half-order peaks. (*c*) AFM image for same sample.

the high quality of the growing layers. The electron diffraction pattern was taken after annealing to ensure proper morphological quality, and is shown in figure 1(*b*). The specular, (0 0), and off-specular, (0 1), (0 −1), and half order (indicated by arrows), $(0\,\frac{1}{2})$, $(0\,-\frac{1}{2})$, Bragg reflections are evident with a streaking pattern characteristic of excellent surface morphology. The half-order peaks are due to the expected structural distortion of the orthorhombic structure [47]. For films of such small thickness, ∼6 nm, AFM imaging is necessary to confirm the sample grows with a uniform surface, as any deviation from 2D growth will lead to a drastically higher surface to volume ratio which could have an adverse effect on materials properties. Figure 1(*c*) displays a 2 × 2 μm^2 AFM scan, showing the high morphological quality of these films, yielding an average surface roughness of <0.7 Å, well below the 3.8 Å BLC.

In addition, the structural properties were investigated by x-ray scattering in the x-ray Diffraction Facility at Northwestern University using Cu K_{α_1} focused radiation with a 4-circle diffractometer; figure 2 displays the x-ray diffraction along the (0 0 2) crystal truncation rod obtained in the vicinity of the YAP (2 2 0) Bragg peak. The sharp peak at Q_z = 3.384 Å^{-1} is the YAP (2 2 0) substrate Bragg peak and the broad feature at Q_z = 3.24 Å^{-1} is the (2 2 0) peak for the ENO film. The analysis of the Bragg peaks from the ENO epitaxial film yields the *c*-axis lattice constant of ENO to be 3.878 Å; in very good agreement with the expected tetragonal expansion from the bi-axial strain and confirms the 15 uc thickness, corroborating the RHEED intensity oscillations for

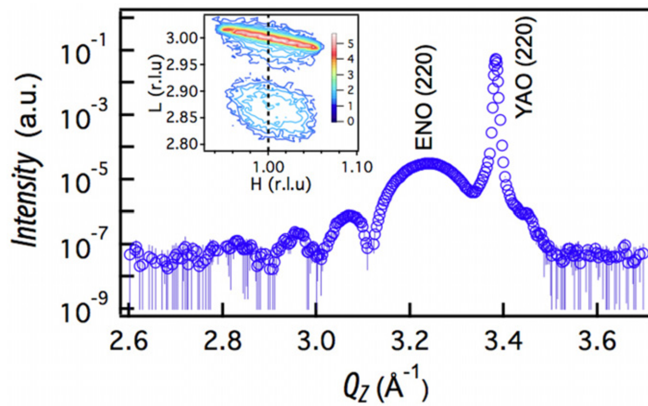

Figure 2. XRD around the (0 0 2) truncation rod of YAP. ENO film peak with thickness fringes is present at lower Q_z. Inset displays the RSM around the (1 0 3) truncation rod, showing the film is fully coherent with the substrate.

layer-by-layer growth (15 pulse trains yielding 15 dips and subsequent recoveries were observed). Additionally, thickness fringes testify for the excellent flatness of the film interfaces and confirm the thickness calculated from the Bragg peak. The reciprocal space map around the off-specular (1 0 3) Bragg intensity for the film and the substrate is also shown in the inset of figure 2. The position of the weak ENO (1 0 3) peak relative to the YAP (1 0 3) peak confirms that the ENO epitaxial thin film is coherently strained to the substrate. XRD survey scans did not reveal the presence of any impurity peaks, such as the typically problematic and thermodynamically more stable NiO (not shown). However, for such thin films detection of a small amount of impurity, especially considering it has no reason to be preferentially oriented relative to the substrate, is very difficult. In order to confirm the lack of NiO impurity and confirm the Ni^{3+} valence necessary for material properties, spectroscopic measurements were needed.

To investigate the electronic and chemical structure of these films, XAS measurements on the Ni L-edge were obtained in both total electron yield (TEY) and total fluorescence yield (TFY) modes in the soft x-ray branch at the 4-ID-C beamline at the Advanced Photon Source in Argonne National Laboratory. The penetration depth of x-rays in TEY mode (∼12 nm) is larger than the film thickness (∼6 nm) allowing it to be used with ambiguity between the surface and bulk signal. The results of the experiment are shown in figure 3 along with absorption on the reference bulk NNO powder. As seen, the line-shape and position of the Ni L_2-edge located at 870.5 eV very closely resembles that of the NNO powder, which shares the Ni^{3+} state, testifying that the 3+ valence state of Ni was obtained, confirming that the proper ENO stoichiometry crucial for materials quality was achieved [48]. This measurement also excludes the possibility of any low concentration NiO impurity phase not detectable by XRD, as the Ni^{2+} would give a separate peak shifted to lower energy on the L_2-edge with a characteristic multiplet structure; a reference NiO is shown in figure 3. This confirms ENO films with the required Ni^{3+} valence and with an absence of the problematic NiO impurity phase were obtained.

In conclusion, high quality ultra-thin ENO films were successfully grown via pulsed laser deposition on YAP substrates. Several characterization tools, including RHEED, AFM, XRD, RSM and XAS were used to investigate sample structural, electronic and chemical properties. These measurements revealed the samples exhibited high morphological quality, high structural quality, fully epitaxial strain, proper stoichiometry, and no impurity phases. The ability to grow the more highly distorted nickelates opens a promising avenue in the study of the physics of the correlated oxide nickelates, allowing separate study of the MIT and AFM, thus disentangling the physics driven by spin and charge ordering.

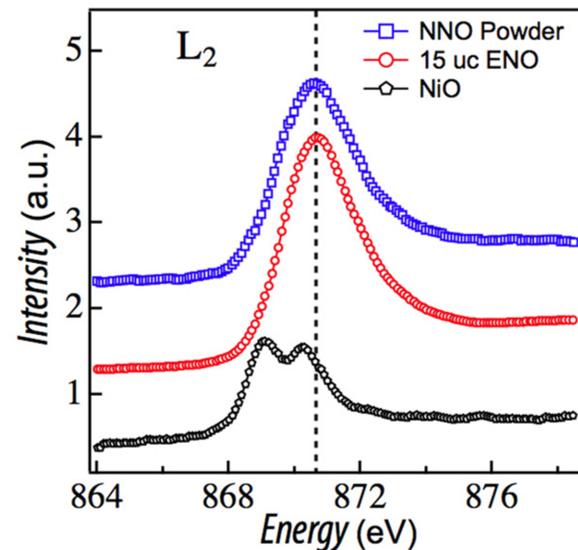

Figure 3. XAS data for ENO sample along with NNO bulk powder and a NiO reference. The strong white line around ∼871 eV indicates Ni^{3+} was obtained. NiO, featuring Ni^{2+}, shows a very dissimilar line shape with a strong peak occurring around ∼869 eV.

Acknowledgments

JC was funded by grants from majority DOD-ARO (W911NF-11-1-0200) and partially NSF (DMR-0747808). Work at the Advanced Photon Source is supported by the US Department of Energy, Office of Science under grant No DEAC02-06CH11357. This work made use of the J B Cohen X-Ray Diffraction Facility supported by the MRSEC programme of the National Science Foundation (DMR-1121262) at the Materials Research Center of Northwestern University.

References

[1] Tokura Y 2003 *Phys. Today* **56** 50–5
[2] Dagotto E 2005 *Science* **309** 257–62
[3] Hwang J, Zhang J Y, Son J and Stemmer S 2012 *Appl. Phys. Lett.* **100** 191909
[4] He J, Borisevich A, Kalinin S V, Pennycook S J and Pantelides S T 2010 *Phys. Rev. Lett.* **105** 227203
[5] Rotella H, Lüders U, Janolin P E, Dao V H, Chateigner D, Feyerherm R, Duzik E and Prellier W 2012 *Phys. Rev.* B **85** 184101
[6] Liu J, Kareev M, Gray B, Kim J W, Ryan P, Dabrowski B, Freeland J W and Chakhalian J 2010 *Appl. Phys. Lett.* **96** 233110

[7] Middey S, Meyers D, Kareev M, Moon E J, Gray B A, Liu X, Freeland J W and Chakhalian J 2012 *Appl. Phys. Lett.* **101** 261602
[8] Chakhalian J *et al* 2011 *Phys. Rev. Lett.* **107** 116805
[9] Liu J, Okamoto S, Veenendaal M van, Kareev M, Gray B, Ryan P, Freeland J W and Chakhalian J 2011 *Phys. Rev.* B **83** 161102(R)
[10] Lim W L, Moon E J,Freeland J W, Meyers D J, Kareev M, Chakhalian J and Urazhdin S 2012 *Appl. Phys. Lett.* **101** 143111
[11] Liu J, Kareev M, Meyers D, Gray B, Ryan P, Freeland J W and Chakhalian J 2012 *Phys. Rev. Lett.* **109** 107402
[12] Stewart M K *et al* 2011 *J. Appl. Phys.* **110** 033514
[13] Scherwitzl R, Gariglio S, Gabay M, Zubko P, Gibert M and Triscone J M 2011 *Phys. Rev. Lett.* **106** 246403
[14] Stewart M K, Liu J, Kareev M, Chakhalian J and Basov D N 2011 *Phys. Rev. Lett.* **107** 176401
[15] Stewart M K *et al* 2011 *Phys. Rev.* B **83** 075125
[16] Han M J, Marianetti C A and Millis A J 2010 *Phys. Rev.* B **82** 134408
[17] Han M J and Veenendaal M van 2011 *Phys. Rev.* B **84** 125137
[18] Veenendaal M Van 2008 *Phys. Rev.* B **78** 165415
[19] Chaloupka J and Khaliullin G 2008 *Phys. Rev. Lett.* **100** 016404
[20] Hansmann P,Yang X, Toschi A, Khaliullin G, Andersen O K and Held K 2009 *Phys. Rev. Lett.* **103** 016401
[21] Imada M, Fujimori A and Tokura Y 1998 *Rev. Mod. Phys.* **70** 1039
[22] Scagnoli V, Staub U, Bodenthin Y, García-Fernández M, Mulders A M, Meijer G I and Hammerl G 2008 *Phys. Rev.* B **77** 115138
[23] Liu J, Kareev M, Gray B, Kim J W, Ryan P, Dabrowski B, Freeland J W and Chakhalian J 2010 *Appl. Phys. Lett.* **96** 233110
[24] Lengsdorf R, Barla A, Alonso J A, Martínez-Lope M J, Micklitz H and Abd-Elmeguid M M 2004 *J. Phys.: Condens. Matter.* **16** 3355
[25] Tiwari A, Jin C and Narayan J 2002 *Appl. Phys. Lett.* **80** 4039
[26] Scherwitzl R, Zubko P, Lezama I G, Ono S, Morpurgo A F, Catalan G and Triscone J 2010 *Adv. Mater.* **22** 5517
[27] Cheng J G, Zhou J S, Goodenough J B, Alonso J A and Martinez-Lope M J 2010 *Phys. Rev.* B **82** 085107
[28] Zhou J S, Goodenough J B and Dabrowski B 2005 *Phys. Rev. Lett.* **95** 127204
[29] Park H, Millis A J and Marianetti C A 2012 *Phys. Rev. Lett.* **109** 156402
[30] Lee S, Chen R and Balents L 2011 *Phys. Rev. Lett.* **106** 016405
[31] Lee S, Chen R and Balents L 2011 *Phys. Rev.* B **84** 165119
[32] Medarde M L 1997 *J. Phys.: Condens. Matter* **9** 1679–707
[33] Caytuero A, Micklitz H, Abd-Elmeguid M M, Litterst F J, Alonso J A and Baggio-Saitovitch E M 2007 *Phys. Rev.* B **76** 193105
[34] Lacorre P, Torrance J B, Panneteir J, Nazzal A I, Wang P W and Huang T C 1991 *J. Solid State Chem.* **91** 225
[35] Alonso J A, Martínez-Lope M J, Casais M T, Aranda M A G and Fernández-Díaz M T 1999 *J. Am. Chem. Soc.* **121** 4754
[36] Torrance J B, Lacorre P and Nazzal A I 1992 *Phys. Rev.* B **45** 8209
[37] Piamonteze C, Tolentino H C N, Ramos A Y, Massa N E, Alonso J A, Martinez-Lopez M J and Casais M T 2002 *Physica* B **320** 71
[38] Kaul A R, Gorbenko O Y and Kamenev A A 2004 *Russ. Chem. Rev.* **73** 861
[39] Lane P A, Crosbie M J, Wright P J, Donohue P P, Hirst P J, Reeves C L, Anthony C J, Jones J C, Todd M A and Williams D J 2003 *Chem. Vapor Depos.* **9** 87
[40] Conchon F, Boulle A, Guinebretière R, Girardot C, Pignard S, Kreisel J, Weiss F, Dooryhée E and Hodeau J 2007 *Appl. Phys. Lett.* **91** 192110
[41] Aydogdu G H, Ha S D, Viswanath B and Ramanathan S 2011 *J. Appl. Phys.* **109** 124110
[42] Zaghrioui M, Bulou A, Lacorre P and Laffez P 2001 *Phys. Rev.* B **64** 081102(R)
[43] Bilewska K, Wolna E, Edely M, Ruello P and Szade J 2010 *Phys. Rev.* B **82** 165105
[44] Kareev M, Prosandeev S, Gray B, Liu J, Ryan P, Kareev A, Moon E J and Chakhalian J 2011 *J. Appl. Phys.* **109** 114303
[45] Blank, Koster G, Rijnders G A J H M, Setten E van, Slycke P and Rogalla H J 2000 *Cryst. Growth* **211** 98
[46] Meyers D, Middey S, Kareev M, van Veenendaal M, Moon E J, Gray B A, Liu J, Freeland J W and Chakhalian J 2013 *Phys. Rev.* B **88** 075116
[47] Proffit D L, Jang H W, Lee S, Nelson C T, Pan X Q, Rzchowski M S and Eom C B 2008 *Appl. Phys. Lett.* **93** 111912
[48] Kang J S *et al* 2007 *Phys. Rev.* B **76** 195122